

ULTRASOUND-ASSISTED EXTRACTION AND FORMULATION OF TWEEN 80-CURCUMINOIDS NANO-MICELLES FOR ENHANCED AQUEOUS SOLUBILITY AND STABILITY

Tran Quang Hieu^{a*}, Nguyen Phuong Tuyen^b,
Nguyen Quynh Dao^b, Nguyen Quoc Thang^a, Le Van Tan^a

^a*Faculty of Chemical Engineering, Industrial University of Ho Chi Minh City, 12 Nguyen Van Bao, Hanh Thong Ward, Ho Chi Minh City 700000, Vietnam*

^b*Faculty of Food Technology -Saigon Technology University, Ho Chi Minh City, Vietnam, 180 Cao Lo Street, Chanh Hung Ward, Ho Chi Minh City 700000, Vietnam*

Abstract: Curcuminoids derived from *Curcuma longa* possess potent biological activities; however, their therapeutic utility is severely restricted by poor aqueous solubility and low bioavailability. This study aimed to establish an integrated and optimized protocol for the ultrasonic-assisted extraction (UAE) of curcuminoids and the subsequent fabrication of stable Tween 80-based nano-micelles (MCs). The extraction parameters were optimized using 96 % ethanol at a solid-to-solvent ratio of 1:50 (w/v) and 60 °C for 60 min, assisted by ultrasonication at 525 W for 90 seconds, achieving a high extraction efficiency of 76.9 %. Regarding the formulation of nano-micelles, the optimal conditions were identified as a 3 % Tween 80 concentration coupled with ultrasonic homogenization at 450 W for 150 seconds. The resulting MCs were characterized by a spherical morphology, a narrow particle size distribution ranging from 50 to 80 nm, and a Zeta potential of -16.7 mV, indicating colloidal stability governed by steric hindrance. Remarkably, the micellar formulation enhanced the apparent aqueous solubility of curcuminoids to 3.8 g/L, representing a massive improvement compared to the negligible

*T. Q. Hieu, e-mail: tg61550280@iuh.edu.vn, tranquanghieu@iuh.edu.vn

solubility of native curcumin (~11 ng/L). These findings demonstrate a highly efficient and scalable method to produce water-soluble curcuminoid formulations with enhanced physicochemical stability.

Keywords: *Curcuma longa*; *curcuminoids*; *ultrasonic-assisted extraction*; *nano-micelles*; *Tween 80*; *solubility enhancement*.

Introduction

Curcuminoids, a group of natural polyphenolic compounds primarily extracted from the rhizomes of *Curcuma longa* (turmeric), have garnered significant scientific interest over recent decades due to their diverse and potent biological activities.^{1,2} The principal components of curcuminoids include curcumin (diferuloylmethane), demethoxycurcumin, and bisdemethoxycurcumin, with curcumin constituting the highest proportion (approximately 70–80 %) and being the most extensively studied bioactive compound.³ Numerous *in vitro* and *in vivo* studies have demonstrated that curcuminoids exhibit anti-inflammatory properties through the inhibition of the NF-κB pathway and pro-inflammatory cytokines, potent antioxidant activity via free radical neutralization, and anticancer potential by inducing apoptosis and suppressing tumor cell proliferation.⁴ Additionally, curcuminoids have been reported to possess neuroprotective, antimicrobial, and therapeutic effects in managing chronic conditions such as diabetes and metabolic disorders.⁵

However, despite these promising therapeutic benefits, the clinical and pharmaceutical application of curcuminoids faces significant limitations. Their poor aqueous solubility (approximately 11 ng/mL for pure curcumin) results in drastically low bioavailability,⁶ while instability under light, heat, and alkaline conditions, coupled with rapid hepatic and intestinal metabolism, further diminishes their therapeutic efficacy.⁷ To address these physicochemical challenges, advanced formulation strategies have been

extensively developed, including nanoemulsion systems,^{8,9} liposomes,¹⁰ cyclodextrin complexes,¹¹ gelatin-based carriers,¹² and notably, surfactant-based micellar systems.¹³

Among these strategies, micellar systems, which self-assemble from surfactant molecules in aqueous solutions above the critical micelle concentration (CMC), have emerged as a particularly effective approach to enhance the solubility, stability, and absorption of hydrophobic compounds like curcuminoids.¹⁴ Regarding surfactant selection, Tween (a polysorbate) is widely favored due to its high safety profile, stable micelle formation, and ability to facilitate cellular membrane permeability. Specifically, Tween 80 (polysorbate 80) is commonly selected for its ability to form small micelle sizes (< 20 nm), maintain structural stability in physiological environments, and exhibit excellent biocompatibility.¹⁵ The mechanism of Tween-curcuminoid micelles involves encapsulating curcuminoid molecules within the hydrophobic core, thereby shielding them from degradation and improving aqueous solubility. Furthermore, micelles can enhance intestinal epithelial transport and prolong systemic circulation time.¹⁶ Previous studies have reported that Tween-curcuminoid micellar systems not only significantly improve solubility (up to hundreds of times compared to free curcuminoids) but also maintain or enhance bioactivity while reducing cellular toxicity.^{3,6}

To date, while substantial research has focused on formulating micelles from pure commercial curcumin, limited attention has been given to developing an integrated process that starts directly from the extraction of curcuminoid-rich turmeric. In this study, we aim to establish a comprehensive optimized protocol ranging from the ultrasonic-assisted extraction of curcuminoids from *Curcuma longa* to the subsequent

preparation and characterization of stable Tween-curcuminoid nanomicelles. By systematically optimizing both extraction and formulation parameters, this work demonstrates a scalable method to significantly enhance the aqueous solubility and physicochemical stability of curcuminoid extracts.

Materials and methods

Chemicals and equipment

Curcumin (99 % purity, Sigma-Aldrich) and polysorbate 80 (Tween® 80, Xylong, China) were used as primary materials. Acetic acid and acetonitrile (HPLC grade, Merck Chemicals and Thermo Fisher Scientific), ethanol (96 %), and double-distilled water, along with other necessary reagents, were employed in the experiments.

Key analytical instruments included a high-performance liquid chromatography system with diode-array detection (HPLC-UV, Agilent 1260, USA), a dynamic light scattering particle size analyzer (Horiba SZ-100, Japan), and an ultrasonic processor (VCX 750, USA) for sample preparation and characterization.

Quantitation of curcumin

The total curcuminoids content was quantified by dissolving the sample in ethanol, homogenizing it via vortexing, and filtering through a 0.45 μ m membrane before HPLC analysis. An Agilent 1260 HPLC system with a UV detector and an Eclipse Plus C18 column (4.6 \times 250 mm, 5 μ m; Agilent) was employed. The mobile phase, composed of acetonitrile and 2 % acetic acid (70:30, v/v), was delivered at a flow rate of 0.8 mL/min. Detection was performed at 425 nm with an injection volume of 20 μ L.

Preparation for turmeric extract

Turmeric rhizomes were procured from traditional markets in Chanh Hung Ward, Ho Chi Minh City, Vietnam. After thorough washing and peeling, the inner flesh was thinly sliced and dried at 60 °C to a constant weight, followed by grinding and sieving to obtain turmeric powder.

The extraction procedure was adapted from the method described in our previous study with minor modifications.¹⁷ The general protocol is described as follows (specific parameters were varied during optimization as detailed in the Results section): Typically, 1.0 g of turmeric powder was suspended in 96 % ethanol at a solid-to-solvent ratio of 1:50 (w/v). The mixture was first subjected to ultrasonic treatment using a probe-type processor (VCX-750) at 525 W for 90 seconds to disrupt cell structures, followed by maceration in a temperature-controlled bath at 60 °C for 60 min. After extraction, the mixture was centrifuged twice at 10.000 rpm for 5 min to collect the supernatant. To enhance purity, the extract was passed through a silica gel chromatography column. Finally, the purified curcuminoids solution was concentrated under reduced pressure using a rotary evaporator until a Brix value of 20 was achieved. The total curcuminoid content was quantified via the HPLC-UV method detailed in Section 2.2.

The extraction yield (ER, %) was calculated as the percentage ratio of extracted curcuminoids content to the total curcuminoids content in the turmeric powder (determined by exhaustive Soxhlet extraction). Factors influencing extraction efficiency, including solid-to-solvent ratio, solvent-to-water ratio, maceration time, maceration temperature, and ultrasonic power and duration, were systematically investigated to identify optimal extraction conditions.

Preparation of curcuminoids-loaded nano-micelles (MCs)

A 3 % Tween 80 aqueous solution was prepared by dissolving 3.0 g of Tween 80 in 100 mL of distilled water under heating at 50 °C with magnetic stirring at 300 rpm until complete dissolution. Subsequently, 1.0 g of the curcuminoids extract (Section 2.3) was gradually introduced into the Tween 80 solution. The mixture was then sonicated using a probe-type ultrasonic processor (VCX-750) at 450 W for 150 s, with temperature controlled by immersing the container in an ice-water bath. Finally, the dispersion was centrifuged at 5000 rpm for 5 min to remove any coarse aggregates, yielding the curcuminoid-loaded nano-micelles (MCs).

Key factors influencing the average particle size (Z-average), including Tween concentration (0.5- 4.0 %), ultrasonic power (150-600 W), and sonication duration (30- 180 s), were systematically investigated to determine optimal preparation conditions.

*Characterization of MCs*Particle size and Zeta potential analysis

The average droplet diameter (Z-average) and PDI of the MCs systems were determined using dynamic light scattering (DLS; Horiba SZ-100, Japan). Due to the transparency of the final MCs systems, measurements were based on laser beam scattering intensity-time fluctuations. All analyses were conducted at 25 °C with a 90 ° scattering angle. To ensure reliability and avoid dilution-induced artifacts, samples were analyzed undiluted. Zeta potential, a key indicator of colloidal stability, was also measured using the same instrument.

Transmission electron microscopy (TEM)

The morphology and precise particle size of the MCs droplets were visualized and validated using transmission electron microscopy (Hitachi H-8100, Japan). Samples were diluted 10-fold, and a droplet was placed on a carbon-coated 300-mesh copper grid, air-dried for 30 seconds, and negatively stained with phosphotungstic acid for 10 seconds. The grid was dried overnight prior to imaging to ensure clear structural resolution.

Results and discussion

Validated the quantitation method of curcuminoids

A validated quantitative method, referenced from previous studies,¹⁸⁻²¹ was applied for curcuminoids determination, incorporating parameters such as limit of detection, recovery, and precision. The calibration curve, constructed over a concentration range of 2.0 - 20 mg/L, exhibited excellent linearity ($y = 141.32x - 69.124$; $R^2 = 0.9973$). The limit of detection (LOD) was 0.5 mg/L. Recovery rates ranged from 98.5 % to 103.2 %, confirming high accuracy. Precision, assessed through intra-day and inter-day relative standard deviation (RSD), yielded values of 2.3 % and 4.5 %, respectively. These results demonstrate the method's reliability for accurate curcuminoids quantification.

Factors affecting extraction efficiency

Effect of solid-to-solvent ratio

In solid-liquid extraction, the solid-to-solvent ratio critically influences extraction efficiency, as the dissolution of target compounds is governed by physical diffusion processes. Increasing the solvent volume enhances the concentration gradient between the solid matrix and the

solvent, thereby accelerating mass transfer and improving yield. Particle size reduction (e.g., via grinding) further amplifies this effect by increasing surface area and facilitating solvent permeation. Higher solvent ratios also reduce extraction time due to improved solute solubility and kinetics.²² However, beyond a certain threshold, the yield plateaus as the system approaches saturation, diminishing the concentration gradient and reducing incremental gains. This limitation can be mitigated through multi-stage or discontinuous extraction strategies.²³

As shown in Figure 1A, curcumin (CUR) extraction efficiency increased from 39.5 % to 62.8 % as the solid-to-solvent ratio rose from 1:20 to 1:60 (w/v). The most significant improvement (23.3 %) occurred between ratios 1:20 and 1:50, while further increasing to 1:60 yielded only a marginal gain, indicating near-saturation conditions. The minimal increase at 1:60 may stem from co-extraction of impurities (e.g., polysaccharides, cellulose, proteins, or resins).¹⁷ Comparatively, Bagchi et al.²⁴ reported a lower CUR yield (30.6 %) at a 1:15 ratio over 90 min, while other studies demonstrated superior efficiency at ratios of 1:40–1:60.²⁵ Consequently, a ratio of 1:50 was selected for subsequent studies to reach the maximum yield while minimizing unnecessary solvent use and impurity co-extraction.

Effect of ethanol concentration

Ethanol concentration significantly influences extraction efficiency, as varying concentrations alter solvent polarity, thereby affecting the solubility of target compounds. Optimizing ethanol concentration reduces solvent consumption, minimizes environmental impact, and enhances selectivity for desired solubles. As shown in Figure 1B, ER increased substantially from 7.1 % to 61.3 % as ethanol concentration rose from 20 % to 100 % (v/v). The most notable improvement (32.4 %) occurred

between 40 % and 100 % ethanol, with the highest yield (61.3 %) achieved at 100 % ethanol. This trend is attributed to solvent polarity, governed by dielectric constant and hydrogen bonding capacity. High-polarity solvents (e.g., low ethanol concentrations) promote ion dissociation but are less effective for non-polar compounds like curcumin. Conversely, reduced polarity at higher ethanol concentrations enhances CUR solubility due to its hydrophobic nature.^{26,27} Statistical analysis confirmed significant differences ($p < 0.05$) among all ethanol concentrations tested (20 - 100 %), underscoring the solvent's critical role in extraction efficiency. Supporting these findings, Our previous study. reported a strong correlation between ethanol concentration and DPPH radical scavenging activity, which increased from 32.03 to 91.43 μg Trolox/g dry weight as ethanol concentration rose from 30 % to 100 %, indicating higher CUR extraction.¹⁷ Similarly, Liu et al. (2018) observed a fourfold increase in DPPH activity at 80 % ethanol (87.07 μg Trolox/g) compared to 30 % ethanol (19.4 μg Trolox/g).²⁸ Based on these results, 100 % ethanol 96° was selected as the optimal solvent for curcuminoid extraction, maximizing yield while maintaining efficiency and reproducibility.

Effect of temperature on ER

Temperature significantly influences the extraction process of bioactive compounds. Elevated temperatures enhance diffusion rates, reduce solvent viscosity, improve mass transfer, and facilitate solute mobility, thereby promoting solvent penetration into cellular matrices. However, excessively high temperatures may degrade target compounds or solvents and induce undesirable reactions, complicating the extraction process.²⁹

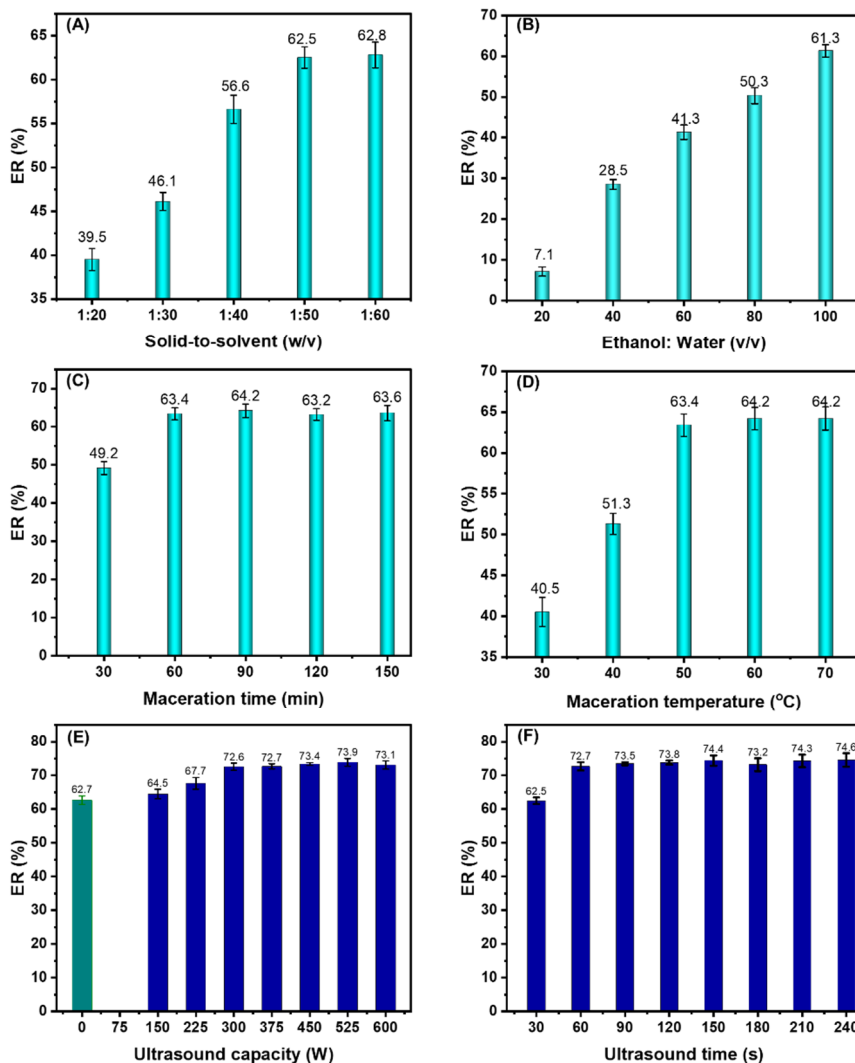


Figure 1. Factors influencing ER: (A) Solid-to-solvent ratio, (B) Solvent-to-water ratio, (C) Maceration time, (D) Maceration temperature, (E) Ultrasonic power, (F) Sonication time.

As shown in Figure 1C, ER % increased from 60.5 % to 64.2 % as temperature rose from 30 °C to 70 °C, peaking at 60 °C (64.2 %). Our previous study previously demonstrated that temperature critically affects CUR extraction and DPPH radical scavenging activity observed at 60 °C and 70 °C compared to lower temperatures (30-50°C). Notably, no

significant difference ($p > 0.05$) was found between 60 °C and 70 °C, leading to the selection of 60 °C as the optimal temperature.¹⁷

Prathapan et al. reported a substantial increase in curcuminoid yield (55–60 %) when extraction temperature was raised from 60 °C to 100 °C for 30 min, with the highest yield (60.11 %) achieved at 80 °C.³⁰ In contrast, Sogi et al. (2010) observed a relatively low CUR extraction efficiency (12.89 %) at 60 °C over 30 min.³¹ These findings align with results from other research groups, supporting the consistency of temperature-dependent extraction trends.³² Thus, 60 °C was identified as the optimal temperature to balance efficiency and compound stability.

Effect of maceration time

Maceration time plays a critical role in determining the extraction efficiency of bioactive compounds from plant materials. Prolonged extraction duration enhances solvent diffusion into cellular structures and improves solute dissolution, thereby increasing yield. However, excessively extended periods may lead to compound degradation due to thermal, photolytic, oxidative, or enzymatic effects, while also promoting the dissolution of undesirable impurities, compromising product purity.³³ Thus, optimizing maceration time is essential to maximize yield while preserving the quality and stability of target compounds.

As illustrated in Figure 1C, ER increased from 49.9 % to 64.1 % as extraction time extended from 30 to 150 min, with the initial 30 minutes yielding 49.9 % and 60 min achieving 63.4 %. Beyond 60 min, yields stabilized with minimal variation, indicating saturation of extractable compounds. Prolonged maceration may adversely affect CUR activity due to factors such as temperature and light exposure. Consequently, 60 min was

identified as the optimal maceration time, balancing extraction efficiency, energy consumption, cost-effectiveness, and compound stability.

Effect of ultrasonic power on ER

Ultrasound waves induce cavitation phenomena, where collapsing vapor bubbles disrupt cell walls, enhance solvent permeation, and improve mass transfer, diffusion, and mixing, thereby increasing extraction efficiency and reducing processing time.³⁴ Ultrasonic power is a critical parameter directly influencing the extraction yield of bioactive compounds from biological materials. Higher power intensifies cavitation, generating stronger pressure waves and microstreaming that facilitate cellular rupture and rapid release of target compounds into the solvent. However, excessive power may cause localized overheating, degradation of heat-sensitive compounds (e.g., curcuminoids, polyphenols), and solvent-derived free radical formation, compromising product quality.³⁵ Thus, optimizing ultrasonic power must balance extraction enhancement with preservation of compound integrity.

As shown in Figure 1D, ultrasonic power significantly influenced the extraction efficiency of curcumin from turmeric powder. With the sonication time fixed at 90 seconds, the baseline yield without ultrasonication (0 W) was 62.7 %. Upon applying ultrasonic energy, the yield exhibited a progressive increase, rising from 64.5 % at 150 W to 72.6 % at 300 W, and eventually peaking at 73.9 % at 525 W. This enhancement is primarily attributed to acoustic cavitation, which disrupts cell walls and facilitates solvent penetration. However, beyond 525 W, the extraction efficiency plateaued, suggesting that the system had reached a saturation threshold. Excessive ultrasonic power may lead to localized overheating and uncontrolled cavitation, potentially degrading heat-sensitive compounds

rather than promoting their release. These results align with our previous study,¹⁷ which reported similar trends where CUR yields increased significantly from 150 W to 525 W before leveling off. Furthermore, antioxidant activity was observed to increase 1.5 - fold with ultrasonication but declined at higher intensities (375–600 W) due to inertial cavitation-induced microstructural damage and free radical generation. Consequently, 525 W was identified as the optimal ultrasonic power to balance extraction efficiency and the preservation of antioxidant activity.

Effect of sonication time on ER

Sonication time significantly influences extraction efficiency, and optimizing this parameter is crucial for minimizing energy costs, solvent usage, and preventing the degradation of bioactive compounds.³⁶ As illustrated in Figure 1F, with the ultrasonic power fixed at 525 W, sonication duration played a pivotal role in the extraction process, exhibiting three distinct phases. Initially, as sonication time increased from 30 to 60 s, extraction efficiency rose sharply from 62.5 % to 72.7 %, demonstrating the strong impact of cavitation-induced cell wall disruption and enhanced solute diffusion. Subsequently, from 60 to 150 seconds, the extraction recovery (ER) increased gradually to 74.4 %, indicating that the majority of extractable compounds had been released. Beyond 150 s, yields plateaued, reaching a maximum of 74.6 % at 240 s, suggesting saturation and diminishing returns.

In our previous work,¹⁷ we observed similar trends, with CUR yields increasing from 66.66 % to 74.72 % as sonication time extended from 30 to 240 seconds. However, prolonged sonication risks energy waste and the degradation of heat-sensitive compounds. Notably, DPPH radical scavenging activity was found to peak at 90 s (139.42 µg Trolox/g dry

weight) before declining at longer durations (129.72 µg Trolox/g at 240 seconds), likely due to thermal effects and free radical generation from water dissociation. Therefore, although extraction yield slightly increased up to 150 seconds, 90 seconds was selected as the optimal sonication time to achieve a high yield while maximally preserving antioxidant activity and reducing operational time.

In summary, the optimal conditions for curcuminoid extraction from turmeric powder are: 96 ° ethanol as solvent, solid-to-solvent ratio of 1:50 (w/v), extraction at 60 °C for 60 min, with ultrasonic assistance (525 W, 90 seconds).

Factors influencing the MCs formation

Effect of Tween 80 concentration

The capacity to generate small-sized micelles during homogenization is contingent upon the nature and concentration of the emulsifier, which plays a pivotal role in stabilizing the system by adequately covering the droplet surfaces.³⁷ The particle size distribution profiles obtained via dynamic light scattering (DLS) are illustrated in Figures 2 (A-E), while the quantitative data and the overall trend regarding Z-average and Polydispersity Index (PDI) are summarized in Table 1.

The data indicate a significant dependence of particle size on surfactant concentration. At lower concentrations (0.5 % and 1.0 %), the DLS profiles exhibited broad peaks (Figures 2A and 2B), corresponding to large hydrodynamic diameters (1296.0 nm and 949.3 nm, respectively) and high PDI values. As the Tween 80 concentration increased, a progressive reduction in particle size was observed, reaching a minimum of 110.0 nm at 3 % with a narrow, monomodal distribution (Figure 2D). However, upon

increasing the concentration to 4 % (Figure 2E), the particle size exhibited negligible change (112.0 nm). This suggests that optimal stabilization was achieved at 3 %.

The observed variations in particle size and distribution can be elucidated by the underlying interfacial phenomena described by McClements (2010).³⁸ According to this theory, droplet formation is governed by a competitive kinetic process between the rate of surfactant adsorption to the interface and the frequency of droplet collisions. At low concentrations, the quantity of surfactant molecules is insufficient to rapidly and fully saturate the newly formed oil-water interface. Consequently, the uncovered droplets are prone to coalescence before they can be stabilized, resulting in larger particle sizes and a broader distribution as observed. This inadequate coverage fails to prevent the rapid coalescence of droplets and Ostwald ripening, resulting in the broad size distributions observed in Figures 2A-B.

Conversely, as the concentration approaches 3.0 %, the ample supply of Tween 80 accelerates the adsorption rate, allowing the emulsifier to rapidly coat the droplet surfaces. Being a non-ionic surfactant with bulky polyoxyethylene head groups, Tween 80 provides significant steric hindrance, preventing droplets from merging. This mechanism explains the sharp decline in particle size and the achievement of the lowest PDI (0.276), indicating a highly monodisperse and stable system. However, the plateau observed in Figure 2F at 4.0 % indicates that increasing the concentration further does not yield size reduction benefits. This aligns with the findings of Tran et al., who noted that exceeding the optimal threshold leads to diminishing returns due to diffusion and adsorption limits.⁹ Furthermore, the slight increase in PDI at 4 % suggests that excess unabsorbed surfactant

molecules in the continuous phase may form free micelles. These micelles can induce depletion forces, potentially causing weak flocculation or thermodynamic instability, thereby confirming that 3 % is the critical threshold for balancing efficient surface coverage and dispersion homogeneity.

Table 1. Average particle size of nanocurcumin according to Tween 80 concentration.

Tween 80 Concentration (%)	Z-average (nm)	PDI
0.5	1296.0 ± 65.6	0.458 ± 0.09
1.0	949.3 ± 13.5	0.562 ± 0.08
2.0	225.7 ± 15.5	0.432 ± 0.08
3.0	110.0 ± 12.0	0.276 ± 0.06
4.0	112.0 ± 12.6	0.318 ± 0.04

In terms of comparative efficacy, the optimal particle size achieved in this study demonstrates distinct advantages over recent reports. Notably, Nguyen et al. (2025) recorded a larger average size of 103 nm using 5 % Tween 40 under similar ultrasonic conditions, suggesting the superior emulsifying efficiency of Tween 80 in this specific formulation.³⁹ Furthermore, the MCs fabricated herein exhibit dimensions that are highly comparable to other carrier systems. For instance, Nguyen et al. reported curcumin-loaded liposomes ranging from 80 to 120 nm. The current MC system consistently falls within or even below this range, achieving these nanoscale dimensions without the need for the complex and costly preparation associated with lipid bilayers.¹⁰

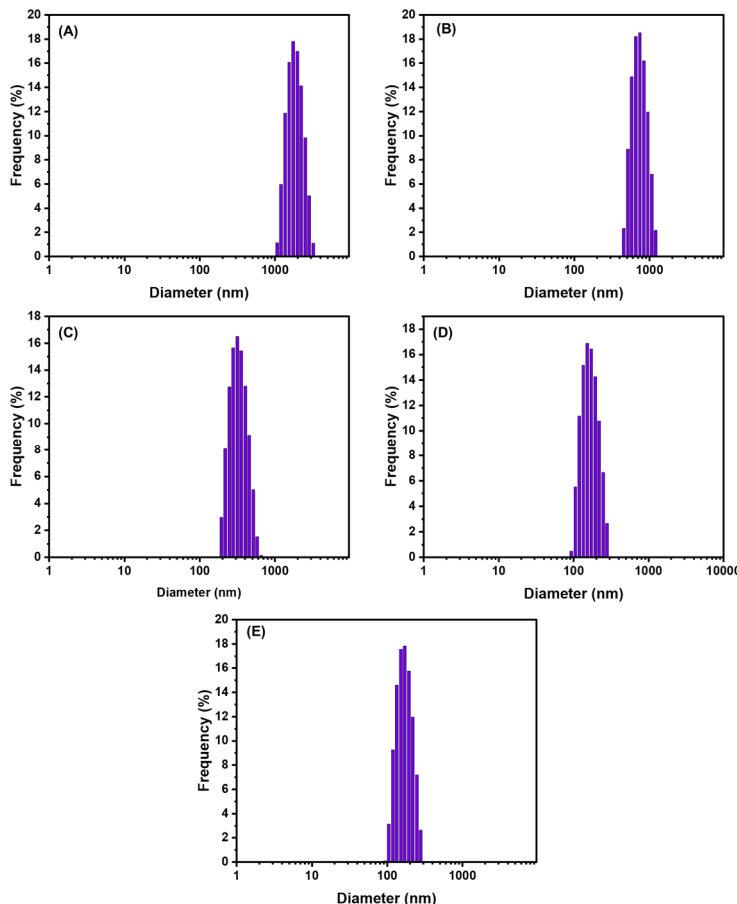


Figure 2. Effect of Tween 80 concentration on the particle size of MCs. (A)–(E) Particle size distribution profiles (determined via DLS) at Tween 80 concentrations of 0.5 %, 1.0 %, 2.0 %, 3.0 %, and 4.0 %, respectively.

Effect of ultrasonic capacity

The influence of ultrasonic power on the nanocurcumin formation process is detailed in Figure 3A. The results demonstrate that ultrasonication is a highly effective method for particle size reduction. Specifically, increasing the power from 150 W to 600 W resulted in a significant decrease in the average particle size from 401 nm to 72 nm. Notably, no statistically significant difference in particle size was observed

between 450 W and 600 W, suggesting that 450 W is sufficient to achieve optimal dispersion.

The mechanism of size reduction can be explained by the acoustic cavitation theory described by C. Devos et al.⁴¹ Low-frequency ultrasound (20-100 kHz) induces instability at the oil-water interface, causing the rapid disruption of the dispersed phase into the continuous phase. Furthermore, the cavitation phenomenon involves the formation, growth, and implosive collapse of microbubbles during alternating compression and rarefaction cycles. The collapse of these bubbles generates intense localized shear forces and turbulence, which continuously disrupt droplets and enhance their contact with the continuous phase, thereby minimizing particle size.

However, the benefits of increasing ultrasonic power are limited by a saturation threshold. Particle size reaches a minimum at a specific energy level, after which it may increase if power is further elevated. At high power levels over a prolonged period, cavitation becomes saturated; bubble formation diminishes while agitation dominates. Under these conditions, the generated Bjerkenes forces drive emulsion droplets toward nodal points where they accumulate. This proximity facilitates coalescence due to the "over-processing" phenomenon, leading to an increase in particle size.⁴¹ These findings align with previous studies regarding the dependency of particle size on ultrasonic power. For instance, Thuy et al. (2019) reported a mean nanocurcumin particle size of 58 nm at 450 W (20 kHz).⁴³ Similarly, Tran et al (2023) and Tan et al. (2025) confirmed that ultrasonic power significantly influences the dimensions of nanoemulsions containing bioactive compounds.^{39,43}

Effect of ultrasonic time

The duration of ultrasonication exhibits a distinct correlation with the dimensional uniformity and stability of MCs. Figure 3B illustrates the effect of ultrasonic time to mean diameter. As the ultrasonic time increased from 30 seconds to 150 seconds, the average particle size decreased continuously from 124 nm to 70.3 nm, accompanied by a reduction in the

standard deviation (SD) from 4.5 to 2.16. This trend reflects the progressive efficiency of the dispersion and stabilization process, driven by cavitation effects and shear forces that disrupt large droplets into homogeneous nanoparticles. However, extending the time to 180 seconds resulted in negligible changes in particle size (70.2 nm) with a sustained low SD, indicating that the system had reached a steady state. Consequently, 150 s was identified as the optimal ultrasonication time to achieve minimal particle size and high stability, as prolonged processing provides no further benefits due to energy limits and cavitation saturation.

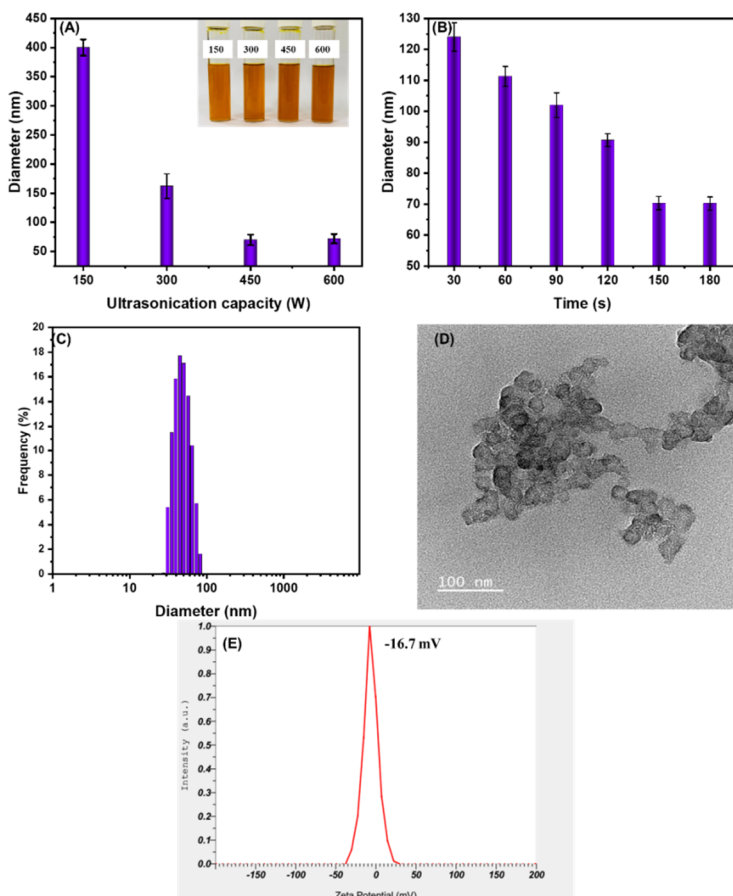


Figure 3. (A) Effect of ultrasonic power on MC particle size; (B) Effect of ultrasonic time on MC particle size; (C) Particle size distribution profile; (D) TEM image showing

spherical morphology; and (E) Zeta potential distribution of the optimal MCs system (at 450 W, 150 s, 3 % Tween 80, and 1.0 % curcuminoids extract).

Physicochemical characterization of MCs

The physicochemical attributes of the synthesized MCs were elucidated through TEM imaging, Zeta potential measurements, and solubility analysis.

As presented in Figure 3C, the synthesized MCs exhibited nanoscale dimensions ranging from 50 to 80 nm, a result that is visually corroborated by the TEM micrograph in Figure 3D. This specific size range is critical, as particles below 100 nm are less susceptible to gravitational separation and Brownian motion dominates, thereby maintaining the system in a suspended state.

Regarding colloidal stability, although Tween 80 is a non-ionic surfactant that primarily stabilizes droplets via steric hindrance, the system exhibited a Zeta potential of -16.7 mV as shown in Figure 3E. This negative surface charge provides a degree of electrostatic repulsion between particles, which complements the steric barrier formed by the polyoxyethylene chains. Consequently, the high colloidal stability of the MCs is attributed to a synergistic mechanism involving both steric hindrance and electrostatic repulsion, preventing particle aggregation and ensuring dispersion uniformity. These findings are consistent with the research of Sahu et al.⁴⁵ who also employed Tween 80 to fabricate stable curcumin-loaded micelles and niosomes.

A remarkable improvement in aqueous solubility was achieved through the micellar encapsulation process. With a loading capacity of 1.0 g of extract per 100 g of water, the apparent solubility of curcumin in the optimized MC system reached 3.8 mg/mL. This represents a massive

enhancement compared to the negligible intrinsic solubility of native curcumin (approximately 11 ng/L). To contextualize this efficiency, these results were compared with previous reports utilizing surfactant-based systems. For instance, prior studies on Tween 20 formulations indicated that curcumin dissolution peaked at only 2.13 mg/mL, even when utilizing a higher surfactant concentration of 4 % w/v.⁴⁵ Furthermore, Inchai et al. (2015) investigated the solubilizing capacity of various polysorbates at a significantly higher concentration of 20 %. They reported that Tween 80 achieved a solubility of approximately 3.4 mg/mL under standard conditions and increased to 4.0 mg/mL only after harsh autoclave treatment⁴⁶. Notably, the present study achieved a comparable and highly competitive solubility of 3.8 mg/mL using a significantly lower surfactant concentration (only 3 % Tween 80 compared to the 20 % used by Inchai et al. without requiring thermal stress. This superior efficiency suggests that the specific combination of high-intensity ultrasonication and optimized Tween 80 concentration effectively facilitates the deep incorporation of hydrophobic curcumin molecules into the micellar core. Consequently, this MC formulation offers a substantial advantage for applications in food, cosmetics, and pharmaceuticals, where reducing surfactant load while maximizing bioavailability is a critical objective.

Conclusion

This study successfully established an integrated and optimized process combining ultrasonic-assisted extraction with a specific surfactant-based micellization technique to produce high-quality curcuminoid nano-micelles from *Curcuma longa*. The extraction process was maximized using 96 % ethanol at a solid-to-solvent ratio of 1:50 (w/v) and 60 °C, assisted by

ultrasonication at 525 W for 90 seconds, followed by a 60 - min maceration. These optimized conditions yielded a high extraction efficiency of 76.9 %. Subsequently, the formulation of nano-micelles was refined to overcome the inherent poor solubility of curcuminoids. The optimal formulation was identified at a 3 % Tween 80 concentration using ultrasonic homogenization at 450 W for 150 seconds. The resulting MCs were characterized by a spherical morphology with a narrow size distribution (50 – 80 nm) and good colloidal stability (Zeta potential of -16.7 mV), stabilized primarily by steric hindrance. Most significantly, this micellar system achieved a dramatic enhancement in the apparent aqueous solubility of curcuminoids, reaching 3.8 g/L, which is a massive improvement over the negligible solubility of native curcumin (~11 ng/L). Unlike complex lipid-based carriers, this study demonstrates a cost-effective, scalable, and highly efficient method using a biocompatible surfactant to unlock the therapeutic potential of turmeric extract. These findings suggest that the developed Tween 80-curcuminoid nano-micelles hold great promise for application in aqueous-based pharmaceuticals, functional foods, and high-value cosmeceuticals.

Conflicts of interest

The authors declare that they have no known competing financial interests or personal relationships that could have appeared to influence the work reported in this paper.

References

1. Hewlings, S.; Kalman, D. Curcumin: A review of its effects on human health. *Foods* **2017**, *6* (10), 92. <https://doi.org/10.3390/foods6100092>

2. Rostinawati, T. Review of surfactant use in Curcumin drug delivery system. *J. Kartika Kim.* **2022**, 5(1), 79 – 89.
<https://doi.org/10.26874/jkk.v5i1.96>
3. Hegde, M.; Girisa, S.; BharathwajChetty, B.; Vishwa, R.; Kunnumakkara, A. B. Curcumin formulations for better bioavailability: What we learned from clinical trials thus far? *ACS Omega* **2023**, 8(12), 10713 – 10746.
<https://doi.org/10.1021/acsomega.2c07326>
4. Olivera, A.; Moore, T. W.; Hu, F.; Brown, A. P.; Sun, A.; Liotta, D. C.; Snyder, J. P.; Yoon, Y.; Shim, H.; Marcus, A. I.; Miller, A. H.; Pace, T. W. W. Inhibition of the NF- κ B signaling pathway by the curcumin analog, 3,5-bis(2-pyridinylmethylidene)-4-piperidone (EF31): Anti-inflammatory and anti-cancer properties. *Int. Immunopharmacol.* **2012**, 12(2), 368 – 377. <https://doi.org/10.1016/j.intimp.2011.12.009>
5. Mohajeri, M.; Momenai, R.; Karami-Mohajeri, S.; Ohadi, M.; Raeisi Estabragh, M. A. Curcumin as a natural therapeutic agent: A rapid review of potential clinical uses and mechanisms of action. *Iran. J. Pharm. Res.* **2025**, 24(1), e156983. <https://doi.org/10.5812/ijpr-156983>
6. Lopresti, A. L. The problem of curcumin and its bioavailability: Could its gastrointestinal influence contribute to its overall health-enhancing effects? *Adv. Nutr.* **2018**, 9(1), 41 – 50.
<https://doi.org/10.1093/advances/nmx011>
7. Zheng, L.; Chen, X.; Zheng, L.; Chang, Q.; Qin, Y.; Ding, X.; Zhang, W.; Zhao, P.; Xi, C. Curcumin-loaded WPI-FUC emulsion as a microcapsule core material enhances the applicability and stability of curcumin – preparation and characterization of a new type of microcapsule. *LWT* **2025**, 224, 117854.
<https://doi.org/10.1016/j.lwt.2025.117854>
8. Tran, Q. H.; Thuy, T. T. H.; Nguyen, T. T. T. Fabrication of a narrow size nano curcuminoid emulsion by combining phase inversion temperature and ultrasonication: Preparation and bioactivity. *New J. Chem.* **2021**, 45(21), 9658 – 9667. <https://doi.org/10.1039/d1nj01241j>
9. Tran, Q. H.; Le Thi, T. T.; Nguyen, T. C.; Tran, T. V.; Le, Q. T.; Luu, T. T.; Dinh, V. P. Facile synthesis of novel nanocurcuminoids–sacha inchi oil using the phase inversion temperature method: Characterization and

antioxidant activity. *J. Food Process. Preserv.* **2021**, *45*(5), e15402. <https://doi.org/10.1111/jfpp.15402>

10. Nguyen, Q. D.; Tran, K. H.; Nguyen, B. T.; Nguyen, P. T.; Nguyen, M. H.; Tran, Q. H. Novel advanced nanoliposomes incorporating adenosine, cordycepin from riched-*Cordyceps militaris* extract, and curcumin: formulation, stability, *in vitro* digestion, and enhanced biological activities. *Food Bioprod. Process.* **2025**, *154*, 334 – 349. <https://doi.org/10.1016/j.fbp.2025.10.006>

11. Jiang, L.; Xia, N.; Wang, F.; Xie, C.; Ye, R.; Tang, H.; Zhang, H.; Liu, Y. Preparation and characterization of curcumin/β-cyclodextrin nanoparticles by nanoprecipitation to improve the stability and bioavailability of curcumin. *LWT* **2022**, *171*, 114149. <https://doi.org/10.1016/j.lwt.2022.114149>

12. Pham, D. C.; Du Cao, V.; Hoang, A. Q.; Nguyen, T. P.; Tran, Q. H.; Nguyen, H. D.; Pham, B. A.; Nguyen, D. T.; Tran, N. Q.; Le Thi, P. Gelatinized-polyoxyethylene (100) stearyl ether nanoformulation for enhancing distribution, bioavailability and stability of curcumin in cancer therapy. *Macromol. Res.* **2025**, *33*(10), 1375 – 139. <https://doi.org/10.1007/s13233-025-00421-7>

13. Wang, G.; Sukumar, S. Characteristics and antitumor activity of polysorbate 80 curcumin micelles preparation by cloud point cooling. *J. Drug Deliv. Sci. Technol.* **2020**, *59*, 101871. <https://doi.org/10.1016/j.jddst.2020.101871>

14. Karjiban, R. A.; Basri, M.; Rahman, M. B. A.; Salleh, A. B. Structural properties of nonionic Tween80 micelle in water elucidated by molecular dynamics simulation. *APCBEE Procedia* **2012**, *3*, 287 – 297. <https://doi.org/10.1016/j.apcbee.2012.06.084>

15. Maher, S.; Geoghegan, C.; Brayden, D. J. Safety of surfactant excipients in oral drug formulations. *Adv. Drug Deliv. Rev.* **2023**, *202*, 115086. <https://doi.org/10.1016/j.addr.2023.115086>

16. Wang, J.; Ma, W.; Tu, P. The mechanism of self-assembled mixed micelles in improving curcumin oral absorption: *In vitro* and *in vivo*. *Colloids Surf. B Biointerfaces.* **2015**, *133*, 108 – 119. <https://doi.org/10.1016/j.colsurfb.2015.05.056>

17. Tran Quang Hieu, N. V. H. Optimizing the process of extracting curcumin from *Curcuma Longa* L. with the aid of ultrasonic waves. In

The first international conference on advanced technology in food science and biotechnology, BFIC; Vietnam Science and Technics Publishing House, 2018; pp 18 – 29.

18. Hieu-Tran, Q. Validation of the method for determination of melamine and investigation its trace in milk from Vietnam by LC-MS/MS. *Asian J. Appl. Chem. Res.* **2021**, 8(1), 13 – 19.
<https://doi.org/10.9734/ajacr/2021/v8i130182>

19. Tran, Q. H.; Pham, K. P.; Nguyen, T. T; Nguyen, Q. T. Simultaneous determination of acepromazine and atropine residues in porks, livers, kidneys by Ultra-High-Performance Liquid Chromatography-Tandem Mass Spectrometry. *Vietnam J. Chem.* **2021**, 59(3), 331 – 340.
<https://doi.org/10.1002/vjch.202000183>

20. Pham, T. A.; Pham, K. P.; Nguyen, T. T.; Thai, H. T.; Tran, Q. H. Auramine O in food products: improved QuEChERS extraction coupled with UHPLC–MS/MS quantitation. *Acta Chem. Iasi* **2024**, 32(2), 183 – 206. <https://doi.org/10.47743/achi-2024-2-0011>

21. Phung, V.-B.; Le, H.-H.; Nguyen, V.-C.; Tran, Q.-H. Highly Sensitive Detection of Nitrofuran Metabolites in Fishery and Food Products Using UHPLC-MS/MS: Method Development and Validation. *Anal. Bioanal. Chem. Res.* **2025**, 12(4), 377 – 387.
<https://doi.org/10.22036/abcr.2025.521190.2340>

22. Huynh, C. P.; Pham, T. P.; Nguyen, M. K.; Tran, Q. H. Bioactivity of ethanol extracts and liposomal formulations from *Psidium Guajava* leaves: Antioxidant, antibacterial, and α -glucosidase inhibition effects. *Acta Chem. Iasi* **2024**, 32(2), 207 – 236.
<https://doi.org/10.47743/achi-2024-2-0012>

23. Prasad, N. K.; Yang, B.; Zhao, M.; Wang, B. S.; Chen, F.; Jiang, Y. Effects of high-pressure treatment on the extraction yield, phenolic content and antioxidant activity of litchi (*Litchi Chinensis* Sonn.) fruit pericarp. *Int. J. Food Sci. Technol.* **2009**, 44(5), 960 – 966.
<https://doi.org/10.1111/j.1365-2621.2008.01768>

24. Bagchi, A. Extraction of curcumin. *IOSR J. Environ. Sci. Toxicol. Food Technol.* **2012**, 1(3), 1–16. <https://doi.org/10.9790/2402-0130116>

25. Green, C. E.; Hibbert, S. L.; Bailey-Shaw, Y. A.; Williams, L. A. D.; Mitchell, S.; Garraway, E. Extraction, processing, and storage effects on

curcuminoids and oleoresin yields from *Curcuma Longa* L. grown in Jamaica. *J. Agric. Food Chem.* **2008**, *56*(10), 3664 – 3670.
<https://doi.org/10.1021/jf073105v>

26. Jouyban, A.; Soltanpour, S.; Chan, H. K. A Simple relationship between dielectric constant of mixed solvents with solvent composition and temperature. *Int. J. Pharm.* **2004**, *269* (2), 353 – 360.
<https://doi.org/10.1016/j.ijpharm.2003.09.010>

27. Govindarajan, V. S.; Stahl, W. H. Turmeric – chemistry, technology, and quality. *Crit. Rev. Food Sci. Nutr.* **1980**, *12* (3), 199–301.
<https://doi.org/10.1080/10408398009527278>

28. Liu, C.; Yang, X.; Wu, W.; Long, Z.; Xiao, H.; Luo, F.; Shen, Y.; Lin, Q. Elaboration of curcumin-loaded rice bran albumin nanoparticles formulation with increased *in vitro* bioactivity and *in vivo* bioavailability. *Food Hydrocoll.* **2018**, *77*, 834 – 842.
<https://doi.org/10.1016/j.foodhyd.2017.11.027>

29. Nguyen, T. T.; Nguyen, D. V.; Tran, Q. H.; Pham, M. D.; Nguyen, V. M.; Nguyen, T. T.; Tran, C. D.; Nguyen, T. D. Choline chloride based natural deep eutectic solvents coupling with ultra-high performance liquid chromatography-tandem mass spectroscopy for effective extraction and rapid detection of adenosine and cordycepin in *Cordyceps militaris*. *J. Mol. Liq.* **2024**, *397*, 124107.
<https://doi.org/10.1016/j.molliq.2024.124107>

30. Prathapan, A.; Lukhman, M.; Arumughan, C.; Sundaresan, A.; Raghu, K. G. Effect of heat treatment on curcuminoid, colour value and total polyphenols of fresh turmeric rhizome. *Int. J. Food Sci. Technol.* **2009**, *44*(7), 1438 – 1444. <https://doi.org/10.1111/j.1365-2621.2009.01976.x>

31. Sogi, D. S.; Sharma, S.; Oberoi, D. P. S.; Wani, I. A. Effect of extraction parameters on curcumin yield from turmeric. *J. Food Sci. Technol.* **2010**, *47*(3), 300 – 304. <https://doi.org/10.1007/s13197-010-0047-8>

32. Paulucci, V. P.; Couto, R. O.; Teixeira, C. C. C.; Freitas, L. A. P. Optimization of the extraction of curcumin from *Curcuma longa* rhizomes. *Braz. J. Pharmacog.* **2013**, *23*(1), 94 – 100.
<https://doi.org/10.1590/S0102-695X2012005000117>

33. Bhadange, Y. A.; Carpenter, J., and Saharan, V. K. A comprehensive review on advanced extraction techniques for retrieving bioactive

components from natural sources. *ACS Omega* **2024**, 9(29), 31274 – 31297. <https://doi.org/10.1021/acsomega.4c02718>

34. Soria, A. C.; Villamiel, M. Effect of ultrasound on the technological properties and bioactivity of food: a review. *Trends Food Sci. Technol.* **2010**, 21(7), 323 – 331. <https://doi.org/10.1016/j.tifs.2010.04.003>

35. Biswas, R.; Sarkar, A.; Alam, M.; Roy, M.; Mahdi Hasan, M. M. Microwave and ultrasound-assisted extraction of bioactive compounds from Papaya: A sustainable green process. *Ultrason. Sonochem.* **2023**, 101, 106677. <https://doi.org/10.1016/j.ultsonch.2023.106677>

36. Nayak, A.; Shah, A.; Bhatt, S.; Bhushan, B.; Kumar, A.; Gaur, R.; Tyagi, I. Ultrasound and microwave assisted extraction of bioactives from food wastes: An overview on their comparative analysis towards commercialization. *Ultrason. Sonochem.* **2026**, 124, 107712. <https://doi.org/10.1016/j.ultsonch.2025.107712>

37. Xiao, T.; Ma, X.; Hu, H.; Xiang, F.; Zhang, X.; Zheng, Y.; Dong, H.; Adhikari, B.; Wang, Q.; Shi, A. Advances in emulsion stability: A review on mechanisms, role of emulsifiers, and applications in food. *Food Chem. X* **2025**, 29, 102792. <https://doi.org/10.1016/j.fochx.2025.102792>

38. McClements, D. J. Emulsion design to improve the delivery of functional lipophilic components. *Annu. Rev. Food Sci. Technol.* **2010**, 1(1), 241 – 269. <https://doi.org/10.1146/annurev.food.080708.100722>

39. Tan, N. T.; Vuong, P. M.; Dao, N. Q.; Dung, T. C.; Nhan, H. T.; Nhu, P. Q.; Dang, N. D. H.; Hieu, T. Q. Novel double nanoemulsion loading of *Cordyceps militaris* extract: formulation, stability, *in vitro* digestion, and *in vivo* evaluation for regulation of acute lipid disorders. *Food Funct.* **2025**, 16(23), 9080 – 9101. <https://doi.org/10.1039/D5FO03188E>

40. Devos, C.; Bampouli, A.; Brozzi, E.; Stefanidis, G. D.; Dusselier, M.; Van Gerven, T.; Kuhn, S. Ultrasound mechanisms and their effect on solid synthesis and processing: A review. *Chem. Soc. Rev.* **2025**, 54(1), 85 – 115. <https://doi.org/10.1039/D4CS00148F>

41. Sakthipandi, K.; Sethuraman, B.; Venkatesan, K.; Alhashmi, B.; Purushothaman, G.; Ansari, I. A. Ultrasound-based sonochemical synthesis of nanomaterials. In *Handbook of Vibroacoustics, Noise and Harshness*; Springer Nature Singapore: Singapore, 2025; pp. 1117 – 1162. https://doi.org/10.1007/978-981-97-8100-3_58

- 42. Thi Thanh Thuy, H.; Thi Kim Ngoc, P.; Thi Thanh, N. T.; Thi Thanh Truc, H.; Van Hai, N.; Quang Hieu, T. Comparision of curcumin nanoemulsion drops size between hominization and ultrasonication supporting. *JST* **2019**, *39*, 3. <https://doi.org/10.46242/jst-iuh.v39i03.277>
- 43. Tran, Q. H.; Chu, H. K. T.; Nguyen, P. T.; Nguyen, V. M.; Nguyen, Q. T.; Tran, C. D.; Nguyen, T. D. Double nanoemulsion loading betalains extract of beetroot (*Beta vulgaris* L.): Ultrasound-assisted synthesis, storage stability, and antioxidant activity. *ACS Food Sci. Technol.* **2023**, *3*(12), 2229 – 2237. <https://doi.org/10.1021/acsfoodscitech.3c00430>
- 44. Sahu, A. K.; Mishra, J.; Mishra, A. K. Introducing Tween-curcumin niosomes: preparation, characterization and microenvironment study. *Soft Matter* **2020**, *16* (7), 1779 – 1791.
<https://doi.org/10.1039/C9SM02416F>
- 45. Ching, Y. C.; Gunathilake, T. M. S. U.; Chuah, C. H.; Ching, K. Y.; Singh, R.; Liou, N.-S. Curcumin/Tween 20 - incorporated cellulose nanoparticles with enhanced curcumin solubility for nano-drug delivery: Characterization and *in vitro* evaluation. *Cellulose* **2019**, *26* (9), 5467 – 5481. <https://doi.org/10.1007/s10570-019-02445-6>
- 46. Inchai, N. Investigation on solubility and stability of curcumin in aqueous polysorbate micelle. In *Proceedings of 31st The IIER International Conference, Bangkok, Thailand, 2nd Aug. 2015, ISBN: 978-93-85465-65-9*; 2015; pp. 91 – 95.